INTERNATIONAL JOURNAL OF PRECISION ENGINEERING AND MANUFACTURING Vol. 17, No. 12, pp. 1711-1719 DECEMBER 2016 / 1711
DOI: 10.1007/s12541-016-0198-2 ISSN 2234-7593 (Print) / ISSN 2005-4602 (Online)

Development and Analysis of Three-Dimensional (3D) Printed Biomimetic Ceramic

Jung-Seob Lee[1], Young-Joon Seol[2], Min Sung[1], Wonkyu Moon[1], Sung Won Kim[3], Jeong-Hoon Oh[3,#], and Dong-Woo Cho[1,#]

1 Department of Mechanical Engineering, POSTECH, 77, Cheongam-ro, Nam-gu, Pohang-si, Gyeongsangbuk-do, 37673, South Korea
2 Wake Forest Institute for Regenerative Medicine, Wake Forest University School of Medicine, NC27101, USA
3 Department of Otolaryngology–Head and Neck Surgery, The Catholic University of Korea, College of Medicine, 180, Wangsan-ro, Dongdaemun-gu, Seoul, 02559, South Korea
Corresponding Author / E-mail: ojhent@catholic.ac.kr, TEL: +82-2-961-4530, FAX: +82-2-960-4568
E-mail: dwcho@postech.ac.kr, TEL: +82-54-279-2171, FAX: +82-54-279-5419

KEYWORDS: Biomimetic ossicles, 3D printing, FE model, Vibration characteristics, Ossicles, Ceramic ossicles

Many finite element (FE) models have been designed based on geometric information from computed tomography (CT) data, and validated via comparison with experimental results for human cadaver ossicular bones. Here, we describe a novel method for developing and analyzing the biomimetic ceramic ossicles (BCO) in combination with 3D printing technology, and we establish an FE model of the BCO for analyzing vibration performance. Novel biomimetic ceramic ossicles (BCO) made of hydroxyapatite (HA) were fabricated using 3D printing technology, and their vibration properties were measured. We created a 3D model of the BCO using computer-aided design, which corresponds to the ossicular structure and geometry, and created an FE model of the human ossicles via a comparison of experimental and simulated vibrations to investigate the characteristics of the ossicular chain. The FE model was established based on the displacements of the malleus, incus, and stapes, which was analyzed using an externally applied vibrational force.

Manuscript received: March 10, 2016 / Revised: July 28, 2016 / Accepted: July 29, 2016

NOMENCLATURE

CAD/CAM= computer-aided design/computer-aided manufacturing
BCO= biomimetic ceramic ossicles
pMSTL= projection-based microstereolithography
STL= stereolithography
PZT= piezoelectric
PCL= poly-caprolactone
LDV= A laser Doppler vibrometer
IMJ= an incudo-malleolar joint
ISJ= an incudo-stapedial joint
HA= hydroxyapatite

1. Introduction

The ossicular chain connects the air-actuated tympanic membrane with the fluid-filled cochlea. Since direct contact between air and the cochlear fluids of the inner ear would not stimulate the perilymph of the inner ear markedly, the primary function of the ossicular chain in the middle ear is to act as an impedance-matching system between the air and cochlear fluids.[1] In patients with defects of the ossicles, such as total (TORP) or partial (PORP) ossicular replacement prostheses are used widely.[2,3] Conventional ossicular replacement prostheses enable the transmission of sound.[4] However, these prostheses cause complications such as inflammation and erosion or extrusion of the prosthesis due to immune reaction triggered by the foreign material in the prostheses. Prostheses made from biocompatible materials should be developed to reduce complications.[5] Titanium (Ti) and hydroxyapatite (HA) prostheses have relatively low complication rates and improved sound transmission. However, it is very difficult for Ti and HA prostheses to transmit all sound because the shape of the prosthesis is simple.[5,6] In addition, existing prostheses cannot transmit sound at all audible frequencies, because the vibration of the ossicles is affected by many variables, including the frequency characteristics of the mass and the structure of the prostheses.[7]

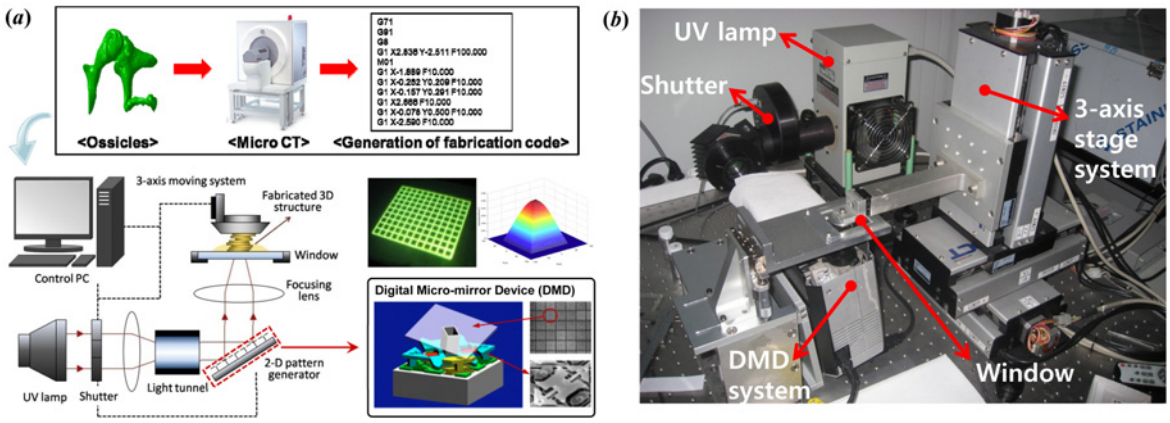

Fig. 1 (a) Schematic diagram of the pMSTL system: cadavaric ossicles were scanned by commputed tomography (CT) and a stereolithography (STL) file was obtained. Fabrication code was generated based on the STL file using in-house software. Using the fabrication code, the biomimetic ceramic ossicles (BCO) was fabricated by pMSTL. (b) A photograph of the pMSTL system used to fabricate the desired three-dimensional (3D) structure from photopolymer resin

In tissue engineering, three-dimensional (3D) printing technology can enable the fabrication of controllable architectures with pre-defined shapes using computer-aided design/computer-aided manufacturing (CAD/CAM). In addition, biomaterials, including bioactive ceramic materials such as hydroxyapatite (HA, Ca10(PO4)6(OH)2), the inorganic component of native bone tissue, can be used with 3D printing to implement bone tissue regeneration, because these materials are biocompatible, biodegradable, and osteoconductive.[8] HA is very effective at inducing the extracellular matrix of bone and the regeneration of native bone tissue, because HA is a component of bone.[9] HA also has relatively good mechanical properties facilitating sound transmission, such as for PORP and TORP with titanium material. However, it is difficult to use ceramics alone as the building material in 3D printing technology, and various fabrication methods have been investigated to fabricate a 3D structure with ceramic as well as biomaterials using fused deposition modeling, selective laser sintering, and stereolithography.[10-13]

The vibration of the ossicles (and of the prostheses) should be analyzed carefully before fabricating advanced prostheses. As such, it is useful to construct a finite element (FE) model of the ossicular chain to evaluate the mechanism affecting vibrations of the ossicles. Numerous studies have reported on FE models of the middle ear, including the ossicles, to investigate the frequency characteristics of the middle ear, including validations of the models via comparison of the displacements of the footplate and umbo with experimental measurements of human cadaver ossicular bones using laser Doppler vibrometry.[14,15] Moreover, the establishment of a delicate experimental model simulating the human ossicles is useful for investigating the vibrational characteristics of the ossicular chain.

Here, we describe a novel method for developing and analyzing the biomimetic ceramic ossicles (BCO) in combination with 3D printing technology, using projection-based microstereolithography (pMSTL) to build a ceramic structure with the desired 3D form, and we establish an FE model of the BCO for analyzing vibration performance. To construct a geometric model of the human ossicles for improved ossicular replacement prostheses, we fabricated an HA ossicular structure imitating the microstructure, geometry, and mechanical properties of natural bone using pMSTL. These BCO emulate the morphological and biological characteristics of the human ossicles, and vibrate in a similar manner. An FE model of a BCO was established by comparison with experimental data, and used to analyze how the BCO vibrated.

2. Materials and Methods

2.1 Projection-based Microstereolithography

Projection-based microstereolithography (pMSTL) was used to fabricate the biomimetic ceramic ossicles, as shown in Fig. 1. This solid freeform fabrication (SFF) technique, which enables fabrication of the desired 3D structures, consists of x-y-z linear stages, an ultraviolet (UV) light (Oriel Research Hg Arc source model 66479; Newport, Irvine, CA), a digital micromirror device (DMD), a controller, and optics for light transfer. The DMD and UV light source generate two-dimensional (2D) patterns, and the 3D structure can be fabricated by stacking the 2D patterns.

2.2 Fabrication of biomimetic ceramic ossicles with hydroxyapatite and PCL using pMSTL

To fabricate the BCO, each ossicle was fabricated individually from commercial hydroxyapatite (HA, Berkeley Advanced Biomaterials, Berkeley, CA) ceramic powder with particles 100 nm in diameter, and ossicles were assembled as shown in Fig. 2. A slurry of 20% hydroxyapatite powder by volume in photo-curable resin (FA1260T; SK-Cytec, Seoul, Korea) was prepared to use the ceramic powder in the pMSTL system because the powder alone is not photo-curable. A 3D computer-aided design (CAD) was generated from cadaveric human ossicles. Using a computed tomography (CT) scanner (7-s scan, resolution: 5 μm thickness) at Seoul St. Mary's Hospital, a stereolithography (STL) file format was obtained at 120 kV and 180 mA. This STL file consisted of about 150000 facets which is a small surface element of 3D model.

Then, 3D CAD model was converted and generated from the STL

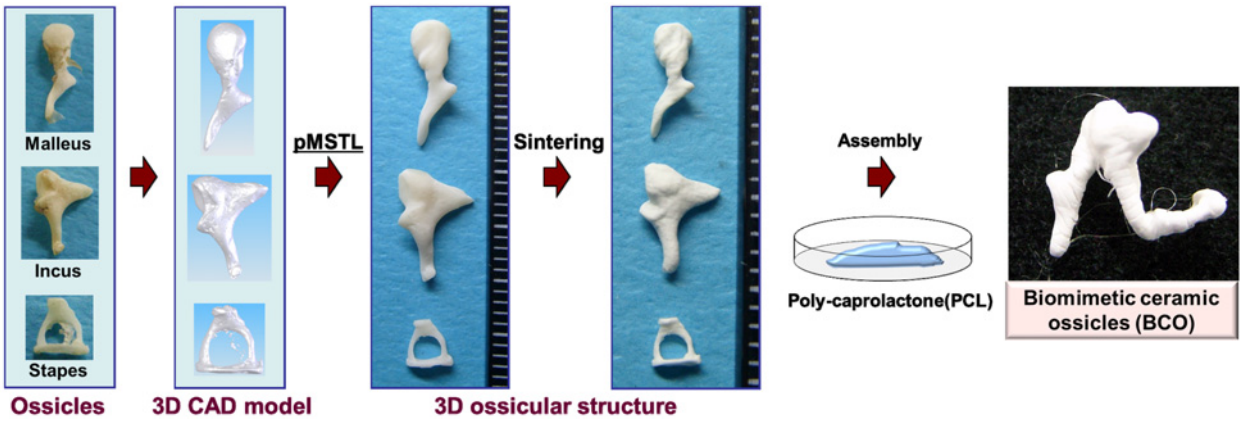

Fig. 2 The fabrication procedure used to form the BCO: A 3D computer-aided design (CAD) model was redesigned based on cadavaric ossicular bones. 3D ossicular structures were fabricated with hydroxyapatite (HA) slurry using pMSTL and the final HA ossicular structures were obtained by sintering. The final HA ossicular structures were assembled with poly-caprolactone (PCL) to give the BCO

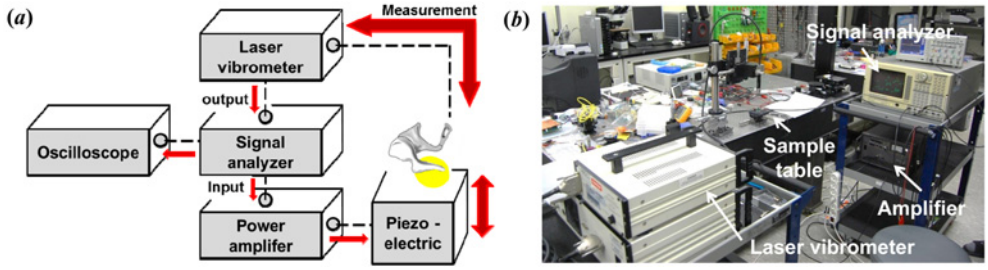

Fig. 3 The vibration measurement system: (a) The schematic diagram shows that the BCO was fixed on piezoelectric (PZT) and the PZT vibrated with the input signal from the signal analyzer. The velocity of the footplate of the BCO was measured by a laser Doppler vibrometer (LDV) and the output data were stored in a signal analyzer. (b) Photograph of the system

file using commercialized CAD software (CATIA V5, Dassault Systemes, Vélizy-Villacoublay, France). The STL model of the human ossicles was divided into 50-μm-thick horizontal slices, and the sliced images were converted into fabrication control data using in-house software.[11,16-19] Using the fabrication control data and pMSTL system, a 3D structure was fabricated. At this step, the 3D structure consisted of hydroxyapatite powder and solidified photo-curable resin. This was sintered in a furnace (LTF15/50/180; Lenton, Hope Valley, Derbyshire, UK) to remove the solidified photo-curable resin and fuse the HA powder particles to one another. We increased the temperature to 1400°C at a rate of 5°C/min and maintained the maximum temperature for 2 hours. In their assembly process, all ceramic ossicles were fabricated and geometrically designed that could fit perfectly with one another. The ceramic ossicles then were assembled to match the middle ear anatomy using poly-caprolactone (PCL, Mw. 43,000~50,000; Polysciences Warrington, PA). Molten PCL served as glue at the designated regions of ceramic structures.

2.3 Evaluation of the vibration of biomimetic ceramic ossicles

The vibration of the BCO was evaluated to confirm that it matched that of human ossicles. Fig. 3 shows the experimental setup used to evaluate the vibration of the BCO. A signal analyzer (Dynamic signal analyzer, SRS-SR785) provided an input signal that activated the vibration source, and this was used to analyze the measured signal.

The power amplifier (HAS 4052) amplified the generated function and transferred it to the vibration source, which consisted of piezoelectric (PZT) lead zirconate titanate (C-91). A specific structure to fix the PZT was designed to minimize experimental noise by pre-stressing it with four bolts, as shown in Fig. 4. A laser Doppler vibrometer (LDV; Polytec OFV 511 and OFV 2700) was used to measure the vibration of the BCO and deliver it to the signal analyzer. When measuring the vibration, the input data comprise a sine wave 50 mV in amplitude with a frequency range of 100–20,000 Hz (frequency resolution, 9.95 Hz); 2000 samples of a magnitude and a phase are taken. The amplified input signal causes the PZT to vibrate up and down. The BCO is attached to the PZT using melted PCL, and the velocity of the BCO is measured with the LDV. The velocity is transferred to the signal analyzer to obtain the output velocity. The experiment was monitored with an oscilloscope. The vibration velocity at points #1 and #2, corresponding to the PZT and the stapes footplate of the BCO, respectively, was acquired to evaluate the vibration performance of the BCO, as shown in Fig. 4.

2.4 Modal analysis of the biomimetic ceramic ossicles using finite element method

Modal analysis of the human ossicles was carried out using the finite element method (FEM), and the results of the modal analysis

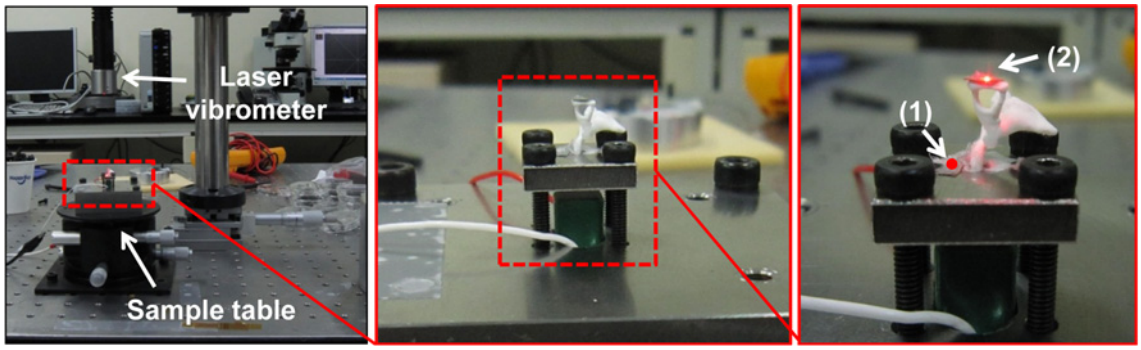

Fig. 4 Evaluation of the BCO using LDV in the experimental vibration measurement system: A laser was focused on points (1) and (2) on the reflective target of the BCO. The velocities of points (1) and (2) were measured and correspond to the input and output data, respectively

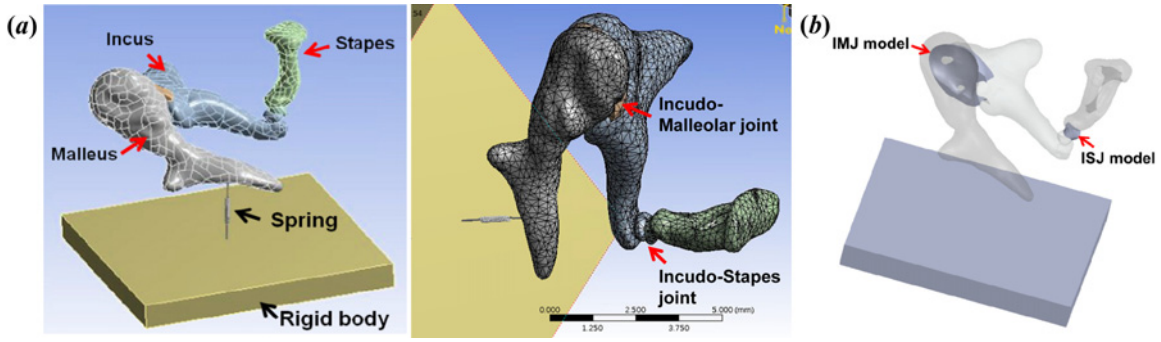

Fig. 5 The 3D finite element (FE) model of the ossicles: Models of the malleus, incus, and stapes were redesigned with CAD based on CT STL files and the incudo-malleolar joint (IMJ) and incudo-stapedial joint (ISJ) were also designed

were compared with those of the experiment. A CAD model of the ossicles was created using SolidWorks (ver. 2010, Dassault Systèmes) (Fig. 5). The STL file format for the CT data of the malleus, incus and stapes was converted into STP file format using Mimics (Materialise, Leuven, Belgium), and the STP files were imported in SolidWorks. The CAD models of the malleus, incus, and stapes were then assembled with an incudo-malleolar joint (IMJ) and an incudo-stapedial joint (ISJ) designed using SolidWorks. For the IMJ design, we created cylindrical structures and obtained the IMJ structure via a Boolean operation considering the size of the cylindrical structure.[20-24] The IMJ structure was redesigned to vibrate with similar resonance frequency to that obtained in experimental results and a final IMJ structure was then determined. We also designed a truncated conical form corresponding to the contact area between incus and stapes for the ISJ structure. The final ISJ structure was obtained via a Boolean operation considering the contact angle between the incus and stapes.[25-27] The 3D models of the IMJ and ISJ are shown in Fig. 5(b). The IMJ and ISJ were modeled as homogeneous isotropic tissue.[20,23,24]

In the native ossicles, the malleus, incus and stapes are bone and the IMJ and ISJ are ligament and tendon. Therefore, the IMJ and ISJ are flexible tissue and the IMJ is tissue that is relatively harder than the ISJ. Upon consideration of the tissue environment, we assumed that the IMJ was relatively hard tissue and that there was little relative motion between malleus and incus at frequencies below 3 kHz.[20-23] The ISJ was formed of relatively flexible tissue, and there was some relative motion between the incus and stapes.[20,25] We determined the material properties of the IMJ and ISJ with PCL using FEM analysis.

Table 1 Material properties of hydroxyapatite and PCL

	Density [kg/m^3]	Modulus [Pa]
Hydroxyapatite	3140	10×10^9
PCL	1145	1.98×10^8

A rigid body and spring were also designed considering the experimental environment (Fig. 5(a)). The vibration source as the PZT in experiment was changed to a rigid body, and the connection between the CAD model of the ossicles and rigid body was simplified using a longitudinal spring. The spring was designed in the following way. In the vibration experiment, PCL was used to bond the BCO and PZT. The connection between the ossicles and rigid body was assumed to be a 1.5 × 1.5 × 1.0-mm rectangular solid based on the experimental environment. In the CAD model, the rectangular solid was represented as a spring. The stiffness of the spring was obtained using Eq. (1) and was used in the FE model.[28]

$$K = \frac{192EI}{c^3} = \frac{192Eab^3}{12c^3} = \frac{16Ea^4}{c^3}, \quad \left(I = \frac{ab^3}{12}\right) \tag{1}$$

where K is the stiffness of the spring, E is Young's modulus, and a, b, and c are the width, length, and height of the rectangular solid, respectively.

Table 1 summarizes the material properties obtained experimentally

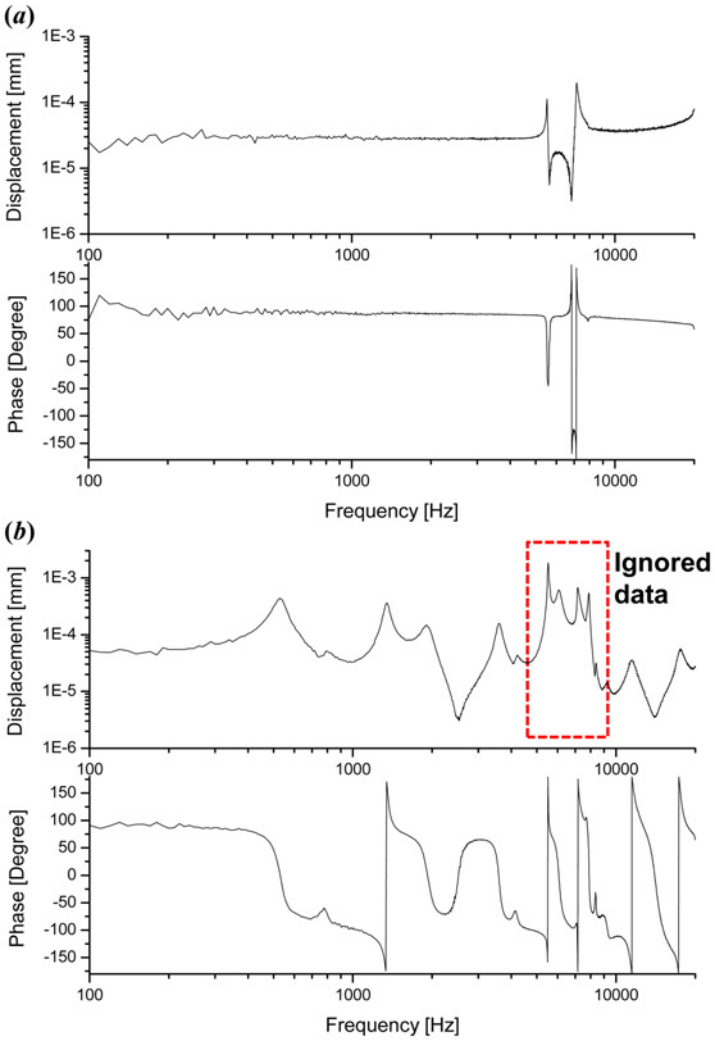

Fig. 6 The experimental vibrational results at locations (a) (1) and (b) (2) shown in Fig. 4. There are two resonances and two anti-resonances in the input data (a). The four resonances of the input data (a) affected the four resonances of the output data (b) at 3-9 kHz (data ignored)

and used in the FEM modal analysis. The material properties of HA and PCL were applied to five parts: HA for the malleus, incus and stapes models, PCL for the malleus-incus and incus-stapes joint models. ANSYS software (Taesung S&E, Korea) was used to conduct the modal analysis of the FE model of the ossicles. A dense tetrahedral mesh was designed (Fig. 5(a)). The six natural frequencies and mode shapes were observed in the range 100-20,000 Hz.

2.5 Harmonic analysis of biomimetic ceramic ossicles using FEM

Harmonic analysis was simulated with ANSYS to obtain frequency-displacement graphs for the malleus, incus, stapes, IMJ, and ISJ. Harmonic analysis is one method to evaluate the degree of vibration of the FE model with an external force based on the natural frequency from the modal analysis. In this study, the vibration behaviors of the malleus, incus, stapes, IMJ, and ISJ were observed over the range 20-100,000 Hz at a sound pressure level (SPL) of 90 dB (0.632 Pa) with the malleus connected to the surface (umbo part) by a spring based on the natural frequency obtained in modal analysis with the BCO FE model.[14,29] The damping ratio was 10^{-6}, which is a basic value for harmonic analysis in ANSYS software.

3. Results

3.1 Fabrication of biomimetic ceramic ossicles using pMSTL

The BCO were fabricated successfully with hydroxyapatite powder using the pMSTL system, as shown in Fig. 2. The shape and dimensions of the BCO were similar to those of actual human ossicles. Shrinkage of about 34% occurred during the sintering process. This was considered when generating the fabrication control data. Then, the individual ceramic malleus, incus, and stapes were assembled with PCL so that the overall shape of the assembled ossicles was similar to that of the chain in the human middle ear.

3.2 Vibration performance characteristics of biomimetic ceramic ossicles

Fig. 6 shows the experimental results obtained using the vibration source and BCO shown in Fig. 4. The graphs use log scales. The vibration source resonated at 5520 and 7170 Hz and showed anti-resonance at 5630 and 6870 Hz, as shown in Fig. 6(a). The BCO resonated at 528, 1344, 1921, and 3584 Hz, as shown in Fig. 6(b). These four frequencies were considered natural frequencies based on

(a)

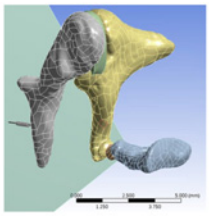

Experimental data		Simulation data	
Resonance Mode	Frequency [Hz]	Resonance Mode	Frequency [Hz]
1	528	1	669.97
2	1344	2	1205.6
3	1921	3	1452.1
4	3584	4	3394.1

(b)

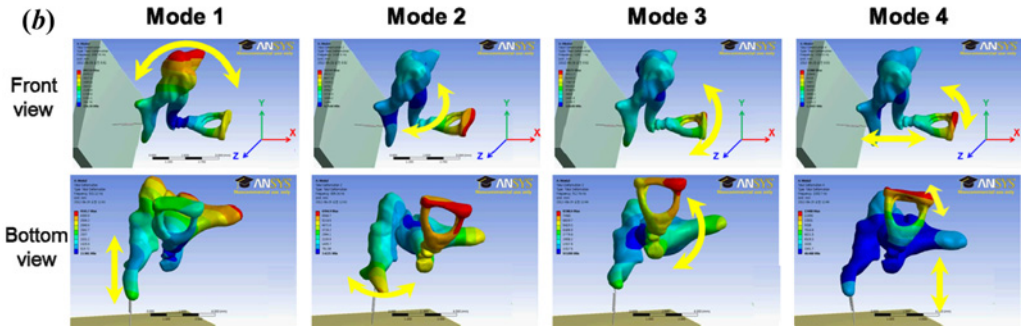

Fig. 7 Results of the modal analysis. (a) The experimental and simulated results were similar, and an FE model of the BCO were established. (b) The mode shapes for the four resonance modes were represented. The vibrational motion of resonance modes 2 and 3 was similar to that of human ossicles

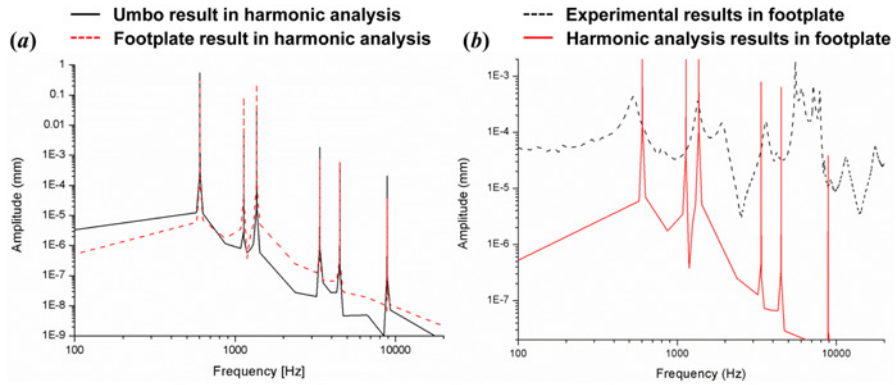

(c)

	Malleus	Incus	Stapes	IMJ	ISJ
Peak Frequency 1	2.5313 mm	2.9451 mm	0.29295 mm	2.2661 mm	0.37344 mm
Peak Frequency 2	0.000615 mm	0.048 mm	0.0848 mm	0.0259 mm	0.0716 mm
Peak Frequency 3	0.10158 mm	0.00502 mm	0.23791 mm	0.03 mm	0.18522 mm
Peak Frequency 4	0.00423 mm	0.00133 mm	0.000785 mm	0.00193 mm	0.00323 mm

Fig. 8 (a) The first peak displacements of the umbo of the malleus and the footplate of the stapes were at 0.6-1.1 kHz and displacements decreased as the frequency increased; (b) Comparison between experimental results of the biomimetic ceramic ossicles and harmonic analysis results of the footplate of the stapes. The first and second peaks of the footplate of the stapes were similar to those in the experimental results; (c) Results of the harmonic analysis using a finite element method for the malleus, incus, stapes, incudo-malleolar joint and incudo-stapedial joint

comparison with the phase results. The four resonances after 3584 Hz were ignored because the natural frequencies of the PZT actuator used as the vibration source vibrated the BCO.

3.3 Modal analysis of biomimetic ceramic ossicles using FEM

Four mode shapes and natural frequencies at 669.97, 1205.6, 1452.1, and 3394.1 Hz were observed in the FEM modal analysis. The resonance frequencies of modes 1, 2, and 4 (669.97, 1205.6, and 3394.1 Hz, respectively) were similar to the experimental results. For each mode shape, the malleus, incus, and stapes models had various movements. In resonance mode 1, the malleus, incus, and stapes vibrated and rotated on the long axis of the malleus (the z-axis in Fig. 7), and the malleus and spring served as a 'hinge.' In resonance mode 2, the ossicular chain vibrated and rotated on the long axis of the stapes (the x-axis in Fig. 7), and the malleus and rigid body vibrated in parallel. In resonance mode 3, the ossicle chain vibrated and rotated on the long axis of the incus and malleus (the y- and z-axes in Fig. 7). In resonance mode 4, the ossicle chain moved straight and vibrated toward the long axis of

the stapes (the x-axis in Fig. 7), while the stapes simultaneously vibrated with rotation on the long axis of the malleus (the z-axis in Fig. 7). The motions of the four mode shapes of the FE model are shown in the supplementary data (Videos #1-4).

3.4 Harmonic analysis of biomimetic ceramic ossicles using FEM

The displacement and phase of each component (malleus, incus, stapes, IMJ, and ISJ) were measured in the x-axis at different frequencies, as shown in Fig. 8. All of the graphs have log scales, and peak displacements occurred at six natural frequencies. All displacements were in range 2.1-4.8 nm at frequencies below 4 kHz, except for the four peak displacement values. The displacement of the second, third, and fourth natural frequencies differed among the malleus, stapes, incus, IMJ, and ISJ. In particular, the magnitudes of the stapes at the second and third natural frequencies were similar, whereas the magnitudes of the incus and malleus displacement were second largest at the second and third natural frequencies, respectively. All of the magnitudes of the ISJ and IMJ were similar to those of the stapes and the average displacement between the malleus and incus, respectively.

4. Discussion

We constructed a BCO prosthesis using the biomaterial HA via 3D printing, and the FE model of the BCO was validated by comparing the experimentally measured and simulated vibrational characteristics of the established BCO model.

The BCO was fabricated via pMSTL using a system developed in house to establish a human ossicles model. The BCO had the same morphological characteristics as human ossicles because the BCO structure was built based on CT data for actual human ossicles as shown in Fig. 2. The BCO also had a similar biological component to human ossicles, because the BCO fabricated by pMSTL was made of hydroxyapatite, which is the major component of bone. The BCO was also non-toxic and biocompatible because it was reported that HA scaffolds fabricated using the same method showed good cell proliferation and biocompatibility.[9] The BCO can be used as an ossicular replacement prosthesis.[30] In addition, it is difficult to fabricate a model of ossicular structures of the desired shape from hydroxyapatite due to its brittle nature.[31,32] Some commercial ossicular prostheses are made of hydroxyapatite to overcome the disadvantages of PORP and TORP, including the side effects of using foreign materials.[21,24] Some researchers have fabricated structures that simply mimic the shape of the ossicles with non-biocompatible materials using a 3D printer. Furthermore, a mimetic ossicular product with non-biocompatible materials was difficult to use in vivo, due to biocompatibility, and did not provide effective sound transmission.[20] In our study, the entire ossicular structure comprising the malleus, incus, and stapes was mimicked using hydroxyapatite slurry by pMSTL. The fabricated ossicular structure composed solely of hydroxyapatite had vibration characteristics similar to those of the natural ossicles based on laser vibrometry. However, one limitation of the study is that we cannot be certain whether the BCO vibrated in exactly the same manner as native human ossicles because we did not directly compare the experimental results for the BCO with real human ossicles by measuring them using the same method.

The estimated natural frequencies of the BCO determined using laser vibrometer were 528, 1344, 1921, and 3584 Hz, with displacement magnitudes ranging from 10^{-3} to 10^{-6} mm. The first three (528, 1344, and 1921 Hz) natural frequencies were regarded as relatively dominant frequencies of the BCO. Several studies have investigated the mechanical behavior of the ossicles at frequencies below 3 kHz.[2,23,33] We focused on three natural frequencies (i.e., 0.5, 1.3, and 1.9 kHz), which were the resonance frequencies of the fabricated BCO. The resonances at 1.3 and 1.9 kHz are similar to the resonance frequency of human ossicles. The resonance frequencies of the human middle ear, which consist of the ossicular chain, ligament and connected tissue to inner ear, are excited by air conduction (AC) or bone conduction (BC). It has been reported that the mean resonance frequency of the middle ear with AC excitation was in the range 1-1.5 kHz.[14] In addition, the resonance frequency of the native ossicular chain is in range of 0.5-2 kHz.[2,33-37] Since the BCO were similar to the native ossicles in both composition and structure, the fabricated and native human ossicles vibrated in a similar manner. For a complete comparison between the BCO and human ossicular chain, more comprehensive comparisons are needed, such as an examination of the vibration mode and resonant frequencies.

The resonance frequency of the first mode (0.5 kHz) was significantly lower than that reported previously. This difference probably resulted from differences in the composition of HA and the structure of bone, as well as the absence of tympanic ligaments of the eardrum, suspensory ligaments and intra-aural tendons attached to the ossicles.[25,29] These attachments increase the stiffness of the ossicles, leading to a higher resonance frequency. Ferris et al. reported that the resonance disappeared altogether if the suspensory ligaments were stiff or slack.[2] Homma et al. reported that different natural frequencies were measured and the ossicular chain behaved differently with the resonant mode in accordance with the ligament.[14] In addition, the effects of the mass of the cochlear fluid were neglected in this study, because we focused on the vibrational characteristics of the BCO, and it is not straightforward to recreate the experimental environment of the cochlear fluid.

In this study, we used FEM to verify the resonant mode of the BCO based on the experimental results. The values of the natural frequencies of the BCO estimated in the modal analysis using FEM were the same as those assessed with LDV. The FEM results showed the vibration motions of the malleus, incus, and stapes at each natural frequency. The simulated natural frequencies of the ossicular chain were in the range 1-2 kHz. When the input frequency was 2 kHz, rotational motion of the malleus and stapes occurs along the long axis of the stapes and malleus (the x- and z-axes as shown in fig. 7(b)).[38] Furthermore, the predominant directions of the movement of the malleus and stapes are inward-outward and upward-downward, as shown in Fig. 7. This movement of the malleus pulled the lenticular process of the incus backwards, and affected the movement of the stapes via a sliding movement of the ISJ.[25]

We performed a harmonic analysis to reveal the vibration characteristics of the ossicular chain and individual ossicles at each natural frequency. We obtained results for the displacement at the umbo of the malleus, part of the incus near the IMJ, the footplate of the stapes, and the entire body of the IMJ and the ISJ, as shown in Fig.

8(c). The direction of all displacements and the phase results paralleled the direction of the vertical plane of the footplate. As the sound was transmitted, the displacements at the malleus and the incus were considerable, the displacement of the ISJ decreased, and the displacement at the footplate of the stapes was relatively small. This was observed at frequencies below 3 kHz and is similar to the typical sound transmission characteristics of the human ossicles.[21,24-27] In particular, the mean displacements of the umbo of the malleus and the footplate of the stapes (see Fig. 8(a)) were similar to those of the human ossicles (i.e., 4.5 nm and 2.5 nm, respectively).[23] Furthermore, the first and second resonance peaks of the umbo at the malleus occurred at 0.6-1 and 1.2-3 kHz, respectively, and the displacement decreased with increasing frequency. Willi et al. reported that the peak displacement of the umbo was at 0.6-1.1 kHz and decreased continuously toward higher frequencies; the second peak, then displacement, occurred at 2-4 kHz. These results are similar.[39] This is similar in frequency to many reports[21-23,39] of sound transmitted from the external ear to inner ear via the displacement of the malleus, incus, and stapes. Moreover, the natural frequencies of the first and second peaks in harmonic analysis were similar to those in the experimental results (see Fig. 8(b)). However, there were slight differences in the magnitude of whole displacement and the third natural frequency between the experimental and harmonic analysis results. This difference was affected by the discrepancy in input data used between the real experiments and the harmonic analysis. Although the natural frequencies of the experimental results did not completely correspond to those of the harmonic analysis, the first, second and fourth natural frequencies were similar. Therefore, we considered that the FE model has been established to understand the behavior of BCO vibration because most tendencies were similar.

The results of the FE vibrational analysis may differ slightly from the behavior of the human's ossicles, because we did not consider the eardrum or joint flexibility, such as suspensory ligaments, or the intra-aural muscle tendons that protect from damage to the inner ear at high frequencies. In the future, the BCO could be used as an ossicular prosthesis for sound transmission if the vibrational characteristics of the BCO are identical to those of human ossicles based on vibration experiments with human ossicles.

5. Conclusion

A ceramic ossicular structure resembling the microstructure and mechanical properties of the human ossicles was fabricated using pMSTL. The natural frequencies of the BCO were measured using LDV, and found to be 528, 1344, 1921, and 3584 Hz. The first three natural frequencies with evident amplitudes (i.e., 528, 1344, and 1921 Hz) were the dominant frequencies of the BCO. FE model, established by comparing these experimental data with a modal analysis, first two resonance modes of the BCO behave similarly to human ossicles. A harmonic analysis revealed discrete vibratory displacement of individual ossicles at each natural frequency. Therefore, we developed a novel method for fabricating a synthetic ossicular chain in the shape of human ossicles and analyze the vibrational characteristics of this artificial ossicular chain. The BCO could be used as an ossicular prosthesis in the foreseeable future.

ACKNOWLEDGEMENT

This work was supported by the National Research Foundation of Korea (NRF) grant funded by the Korea government (MSIP) (No. 2010-0018294).

REFERENCES

1. Volandri, G., Di Puccio, F., Forte, P., and Manetti, S., "Model-Oriented Review and Multi-Body Simulation of the Ossicular Chain of the Human Middle Ear," Medical Engineering & Physics, Vol. 34, No. 9, pp. 1339-1355, 2012.
2. Ferris, P. and Prendergast, P. J., "Middle-Ear Dynamics before and after Ossicular Replacement," Journal of Biomechanics, Vol. 33, No. 5, pp. 581-590, 2000.
3. Mao, M., Zhai, J., Chen, G., Zhang, J., Ma, Z., and Xue, J., "Effect of Ossicular Chain Reconstruction with Titanium Ossicular Replacement Prosthesis in Mastoidectomy with Synchronous Ossiculoplasty," Journal of Clinical Otorhinolaryngology, Head, and Neck Surgery, Vol. 28, No. 10, pp. 708-711, 2014.
4. Wang, X., Hu, Y., Wang, Z., and Shi, H., "Finite Element Analysis of the Coupling between Ossicular Chain and Mass Loading for Evaluation of Implantable Hearing Device," Hearing Research, Vol. 280, No. 1, pp. 48-57, 2011.
5. Nikolaou, A., Bourikas, Z., Maltas, V., and Aidonis, A., "Ossiculoplasty with the Use of Autografts and Synthetic Prosthetic Materials: A Comparison Ofresults in 165 Cases," The Journal of Laryngology & Otology, Vol. 106, No. 8, pp. 692-694, 1992.
6. Yung, M. W., "Literature Review of Alloplastic Materials in Ossiculoplasty," The Journal of Laryngology & Otology, Vol. 117, No. 6, pp. 431-436, 2003.
7. Rosowski, J. J. and Merchant, S. N., "Mechanical and Acoustic Analysis of Middle Ear Reconstruction," Otology & Neurotology, Vol. 16, No. 4, pp. 486-497, 1995.
8. Leong, K. F., Cheah, C. M., and Chua, C. K., "Solid Freeform Fabrication of Three-Dimensional Scaffolds for Engineering Replacement Tissues and Organs," Biomaterials, Vol. 24, No. 13, pp. 2363-2378, 2003.
9. Seol, Y. J., Park, J. Y., Jung, J. W., Jang, J., Girdhari, R., et al., "Improvement of Bone Regeneration Capability of Ceramic Scaffolds by Accelerated Release of their Calcium Ions," Tissue Engineering Part A, Vol. 20, No. 21-22, pp. 2840-2849, 2014.
10. Seol, Y.-J., Kang, T.-Y., and Cho, D.-W., "Solid Freeform Fabrication Technology Applied to Tissue Engineering with Various Biomaterials," Soft Matter, Vol. 8, No. 6, pp. 1730-1735, 2012.
11. Jung, J. W., Kang, H.-W., Kang, T.-Y., Park, J. H., Park, J., and Cho, D.-W., "Projection Image-Generation Algorithm for Fabrication of a Complex Structure Using Projection-based Microstereolithography," Int. J. Precis. Eng. Manuf., Vol. 13, No. 3, pp. 445-449, 2012.

12. Joo, Y.-H., Park, J.-H., Cho, D.-W., and Sun, D.-I., "Morphologic Assessment of Polycaprolactone Scaffolds for Tracheal Transplantation in a Rabbit Model," Tissue Engineering and Regenerative Medicine, Vol. 10, No. 2, pp. 65-70, 2013.

13. Yeong, W.-Y., Chua, C.-K., Leong, K.-F., and Chandrasekaran, M., "Rapid Prototyping in Tissue Engineering: Challenges and Potential," Trends in biotechnology, Vol. 22, No. 12, pp. 643-652, 2004.

14. Homma, K., Du, Y., Shimizu, Y., and Puria, S., "Ossicular Resonance Modes of the Human Middle Ear for Bone and Air Conduction," The Journal of the Acoustical Society of America, Vol. 125, No. 2, pp. 968-979, 2009.

15. Ball, G. R., Huber, A., and Goode, R. L., "Scanning Laser Doppler Vibrometry of the Middle Ear Ossicles," Ear, Nose, & Throat Journal, Vol. 76, No. 4, pp. 213-218, 220, 222, 1997.

16. Shor, L., Güçeri, S., Wen, X., Gandhi, M., and Sun, W., "Fabrication of Three-Dimensional Polycaprolactone/Hydroxyapatite Tissue Scaffolds and Osteoblast-Scaffold Interactions in Vitro," Biomaterials, Vol. 28, No. 35, pp. 5291-5297, 2007.

17. Lee, J. W., Lan, P. X., Kim, B., Lim, G., and Cho, D. W., "Fabrication and Characteristic Analysis of a Poly (Propylene Fumarate) Scaffold using Micro-Stereolithography Technology," Journal of Biomedical Materials Research Part B: Applied Biomaterials, Vol. 87, No. 1, pp. 1-9, 2008.

18. Seol, Y. J., Park, D. Y., Park, J. Y., Kim, S. W., Park, S. J., and Cho, D. W., "A New Method of Fabricating Robust Freeform 3D Ceramic Scaffolds for Bone Tissue Regeneration," Biotechnology and Bioengineering, Vol. 110, No. 5, pp. 1444-1455, 2013.

19. James, M. G., "Mechanics of Materials," Thomson-Engineering, 6th Ed., 2003.

20. Sun, Q., Chang, K.-H., Dormer, K. J., Dyer, R. K., and Gan, R. Z., "An Advanced Computer-Aided Geometric Modeling and Fabrication Method for Human Middle Ear," Medical Engineering & Physics, Vol. 24, No. 9, pp. 595-606, 2002.

21. Onchi, Y., "Mechanism of the Middle Ear," The Journal of the Acoustical Society of America, Vol. 33, No. 6, pp. 794-805, 1961.

22. Møller, A. R., "An Experimental Study of the Acoustic Impedance of the Middle Ear and Its Transmission Properties," Acta Oto-Laryngologica, Vol. 60, No. 1-6, pp. 129-149, 1965.

23. Vlaming, M. S. M. G., "Middle Ear Mechanics by Laser Doppler Interferometry," Ph.D. Thesis, Department of Applied Sciences, Delft University of Technology, 1987.

24. Marquet, J., "The Incudo-Malleal Joint," The Journal of Laryngology & Otology, Vol. 95, No. 6, pp. 543-565, 1981.

25. Hüttenbrink, K.-B., "The Mechanics of the Middle-Ear at Static Air Pressures: The Role of the Ossicular Joints, the Function of the Middle-Ear Muscles and the Behaviour of Stapedial Prostheses," Acta Oto-Laryngologica, Vol. 105, Suppl. 451, pp. 1-35, 1988.

26. Yamada, M., Tsunoda, A., Muraoka, H., and Komatsuzaki, A., "Three-Dimensional Reconstruction of the Incudostapedial Joint with Helical Computed Tomography," The Journal of Laryngology & Otology, Vol. 113, No. 8, pp. 707-709, 1999.

27. Skinner, M., Honrado, C., Prasad, M., Kent, H. N., and Selesnick, S. H., "The Incudostapedial Joint Angle: Implications for Stapes Surgery Prosthesis Selection and Crimping," The Laryngoscope, Vol. 113, No. 4, pp. 647-653, 2003.

28. Goldenberg, R. A. and Driver, M., "Long-Term Results with Hydroxylapatite Middle Ear Implants," Otolaryngology-Head and Neck Surgery, Vol. 122, No. 5, pp. 635-642, 2000.

29. Sun, Q., Gan, R., Chang, K.-H., and Dormer, K., "Computer-Integrated Finite Element Modeling of Human Middle Ear," Biomechanics and Modeling in Mechanobiology, Vol. 1, No. 2, pp. 109-122, 2002.

30. Shor, L., Darling, A., Starly, B., Sun, W., and Guceri, S., "Precision Extruding Deposition of Composite Polycaprolactone/Hydroxyapatite Scaffolds for Bone Tissue Engineering," Proc. of IEEE 31st Annual Northeast Bioengineering Conference, pp. 172-173, 2005.

31. Kim, H.-W., Knowles, J. C., and Kim, H.-E., "Hydroxyapatite Porous Scaffold Engineered with Biological Polymer Hybrid Coating for Antibiotic Vancomycin Release," Journal of Materials Science: Materials in Medicine, Vol. 16, No. 3, pp. 189-195, 2005.

32. Ovsianikov, A., Chichkov, B., Adunka, O., Pillsbury, H., Doraiswamy, A., and Narayan, R., "Rapid Prototyping of Ossicular Replacement Prostheses," Applied Surface Science, Vol. 253, No. 15, pp. 6603-6607, 2007.

33. Nakajima, H. H., Ravicz, M. E., Merchant, S. N., Peake, W. T., and Rosowski, J. J., "Experimental Ossicular Fixations and the Middle Ear's Response to Sound: Evidence for a Flexible Ossicular Chain," Hearing Research, Vol. 204, No. 1, pp. 60-77, 2005.

34. Wada, H., Metoki, T., and Kobayashi, T., "Analysis of Dynamic Behavior of Human Middle Ear using a Finite-Element Method," The Journal of the Acoustical Society of America, Vol. 92, No. 6, pp. 3157-3168, 1992.

35. Wada, H., Koike, T., and Kobayashi, T., "Three-Dimensional Finite-Element Method (FEM) Analysis of the Human Middle Ear," Middle Ear Mechanics in Research and Otosurgery, Dresden, pp. 76-81, 1997.

36. Zwislocki, J., "Some Impedance Measurements on Normal and Pathological Ears," The Journal of the Acoustical Society of America, Vol. 29, No. 12, pp. 1312-1317, 1957.

37. Wada, H., Koike, T., and Kobayashi, T., "Clinical Applicability of the Sweep Frequency Measuring Apparatus for diagnosis of Middle Ear Diseases," Ear and hearing, Vol. 19, No. 3, pp. 240-249, 1998.

38. Berger, E. H., Kieper, R. W., and Gauger, D., "Hearing Protection: Surpassing the Limits to Attenuation Imposed by the Bone-Conduction Pathways," The Journal of the Acoustical Society of America, Vol. 114, No. 4, pp. 1955-1967, 2003.

39. Willi, U. B., Ferrazzini, M. A., and Huber, A. M., "The Incudo-Malleolar Joint and Sound Transmission Losses," Hearing Research, Vol. 174, No. 1, pp. 32-44, 2002.